

# Zinc tetraaminophthalocyanine-Fe<sub>3</sub>O<sub>4</sub> nanoparticle composite for laccase immobilization

Jun Huang  
Cheng Liu  
Haiyan Xiao  
Juntao Wang  
Desheng Jiang  
Erdan GU

Key Laboratory of Fiber Optic Sensing Technology and Information Processing of Ministry of Education, Wuhan University of Technology, Wuhan, Hubei, P.R. China

**Abstract:** Zinc tetraaminophthalocyanine-Fe<sub>3</sub>O<sub>4</sub> nanoparticle composites were prepared by organic-inorganic complex technology and characterized. It has been proved that the ZnTAPc dispersed randomly onto the surface of Fe<sub>3</sub>O<sub>4</sub> nanoparticles to form molecular dispersion layer and there was a relatively strong bond between central zinc cation and oxygen. The nanoparticle composite took the shape of roundish spheres with the mean diameter of about 15 nm. Active amino groups of magnetic carriers could be used to bind laccase via glutaraldehyde. The optimal pH for the activity of the immobilized laccases and free laccase were the same at pH 3.0 and the optimal temperature for laccase immobilization on ZnTAPc-Fe<sub>3</sub>O<sub>4</sub> nanoparticle composite was 45°. The immobilization yields and  $K_m$  value of the laccase immobilized on ZnTAPc-Fe<sub>3</sub>O<sub>4</sub> nanoparticle composite were 25% and 20.1 μM, respectively. This kind of immobilized laccase has good thermal, storage and operation stability, and could be used as the sensing biocomponent for the fiber optic biosensor based on enzyme catalysis.

**Keywords:** ZnTAPc-Fe<sub>3</sub>O<sub>4</sub> nanoparticles composite; organic-inorganic complex; laccase immobilization

## Introduction

Fiber optic biosensor has many advantages such as high sensitivity, fast response, low cost, immunity from electrical and magnetic disturbances, geometrical versatility, remote sensing capability, small size and lightweight, and can provide an alternative to laboratory-based measurement methods (D'souza 2001; Kishen et al 2003; Cooper et al 2004). Fiber optic biosensors are composed of a biological recognition element (biocomponent), a transducer to convert the biocomponent response to an optical signal and associated electronics. Laccases (EC 1.10.3.2) are copper oxidoreductases produced by higher plants and micro-organisms, mainly fungi. For the fiber optic biosensors based on laccase catalysis which have great application in clinical medicine detection, the immobilized laccase, formed by the immobilization of enzyme on a carrier, could act as the sensing biocomponent and will have tremendous influence to the sensor properties. The immobilization of laccases on various carriers, including activated glass beads, sepharose, gelatin, polyurethane, platinum and organic gels, have been reviewed previously (Duran et al 2002). The use of organic-inorganic magnetic particles as the potential supports appears to be a promising technique (Arica et al 2000; Zheng et al 2003; Liu et al 2004). Some successful applications of magnetic nanoparticles in the biomolecules immobilization have been reported (Chen et al 2002; Li et al 2003). However, the particle size was often of micrometer or millimeter scale for most available magnetic carriers used for the laccase immobilization. Comparing with them, the nanoparticle composites showed an increased surface areato-volume ratio to bind more enzymes and they had a favorable spatial orientation of the enzyme molecule, further more, their superparamagnetism was propitious to separate from solution and reuse.

In our previous study, we used copper tetra aminophthalocyanine (CuTAPc)-Fe<sub>3</sub>O<sub>4</sub> nanoparticle composite with the average size of 76 nm to immobilize laccase (Jun

Correspondence: Jun Huang  
Key Laboratory of Fiber Optic Sensing Technology and Information Processing (Ministry of Education)  
Wuhan University of Technology, Wuhan, 430070, P.R. China  
Tel +86 27 876 51850 ext 8005  
Fax +86 027 876 65287  
Email hjun@whut.edu.cn

et al 2006). The composite showed an increased surface area-to-volume ratio to bind more enzyme and the immobilized laccases had good activity and stability, and could be easily separated from solution for reuse because of the magnetic properties of the carrier. In this paper, ZnTAPc (Zinc tetraaminophthalocyanine)-Fe<sub>3</sub>O<sub>4</sub> nanoparticle composites were prepared in situ by organic-inorganic complex technology and characterized. The laccase was immobilized on the surface of the magnetic composite via glutaraldehyde. The influences of pH, temperature to the activity of immobilized and free laccase were studied and the properties of the immobilized and free laccase such as stabilities, kinetic constants were investigated. Compared with CuTAPc-Fe<sub>3</sub>O<sub>4</sub> nanoparticle composite, ZnTAPc-Fe<sub>3</sub>O<sub>4</sub> nanoparticle composite had even smaller size and larger surface area-to-volume ratio to bind more laccase, which would be beneficial to improve the properties of the fiber optic biosensor based on laccase catalysis.

## Experimental

### Materials and measurement

*Pycnoporus sanguineus* laccase, a white-rot fungus laccase with a molecular weight of 64 kDa, was presented by the Institute of Microbiology of the Chinese Academy of Sciences and its purity was tested by electrophoresis with a single protein band.

The 2,2'-Azino-bis-(3-ethylbenzothiazoline-6-sulphonic acid) (ABTS) was purchased from Sigma Chemical Co. (Deisenhofen, Germany). All other solvents and reagents were of analytical grade and were used without further purification. Water was deionized and doubly distilled prior to use. For the characterization of ZnTAPc-Fe<sub>3</sub>O<sub>4</sub> nanoparticle composite and the immobilized laccase, FTIR (Fourier-transform infrared) spectra were recorded on a Nicolet 60 SXB spectrophotometer (Nicolet, USA). X-ray powder patterns were conducted on a Rigaku D/MAX-RB diffractometer (Rigaku, Japan). XPS (X-ray photoelectron spectroscopy) was performed by INCA energy spectrometer (OXFORD). The morphological characterization of the composite was evaluated by TEM (transmission scanning electron microscopy) (JEM-2000FX $\alpha$ ) operating at 150 kV. The magnetic properties of the composite were determined by Model 4HF VSM (ADE Corp, DMS-Magnetics). The surface area was analyzed by Nova instrument (Quantachrome, USA). The activity of laccase was assayed by using a UV-2450 spectrophotometer (Shimadzu, Japan).

### Preparation of ZnTAPc-Fe<sub>3</sub>O<sub>4</sub> nano composite

The Zinc Tetraaminophthalocyanine (ZnTAPc) was synthesized according to the illustrative scheme shown in

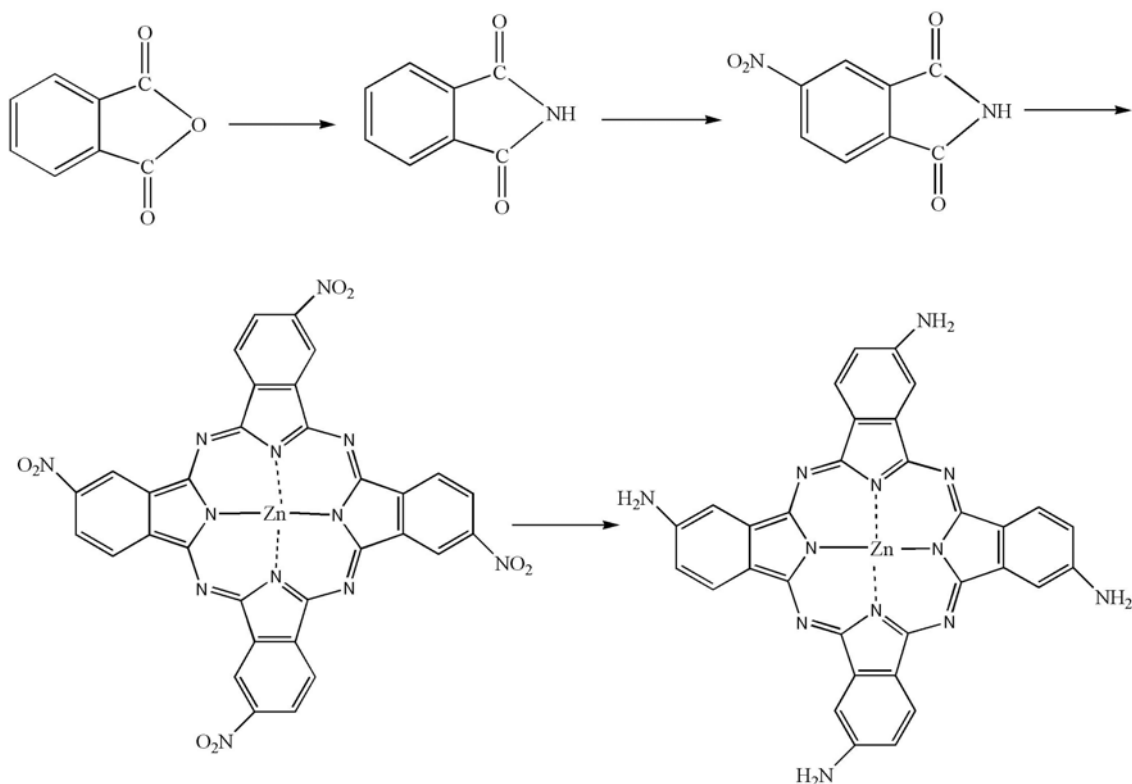


**Figure 1** Schematic illustration of synthesis of ZnTAPc.

Figure 1 described previously (Cong et al 2002). The  $\text{Fe}_3\text{O}_4$  nanoparticles with the average size of 10 nm were prepared by common chemical precipitation as described elsewhere (Huang et al 2001). After the eluate was washed to neutral, 0.97 g of  $\text{Fe}_3\text{O}_4$  nanoparticles were transferred to a suitable organic solvent and then were slowly mixed with 0.03 g ZnTAPc dissolved in N, N-dimethyl formamide (DMF). The mixture was stirred for 24 h at room temperature and then dried under vacuum. After the removal of DMF, the ZnTAPc- $\text{Fe}_3\text{O}_4$  nanoparticle composites were formed. The composites were washed with DMF and almost no free ZnTAPc could be found in the solution, indicating that almost all of the ZnTAPc had been combined with the  $\text{Fe}_3\text{O}_4$  nanoparticles and the content of ZnTAPc was 3% (by weight).

### Laccase immobilization

1 g ZnTAPc- $\text{Fe}_3\text{O}_4$  nanoparticle composites were added in the solution with a certain amount of glutaraldehyde with stirring for 2 h and the excess glutaraldehyde was washed off with distilled water in the presence of a magnetic field. The ZnTAPc- $\text{Fe}_3\text{O}_4$  nanoparticle composite crosslinked with glutaraldehyde were added to 0.1 M phosphate buffer solution (PBS) containing a certain amount of laccase with continuous stirring for 2 h. The immobilized laccase was washed with PBS (pH 7.0) until no protein was detected in the eluate and was then freeze-dried and stored at 4 °C.

### Assay of laccase activity

Activities of immobilized laccase were assayed by using 4 mg/ml ABTS in distilled water as a substrate. The reaction mixture consisting of 3 ml of 0.1 M tartaric acid buffer (pH 3.0) and 15 mg of immobilized laccase was initiated by adding 20  $\mu\text{l}$  of substrate and reacted for 5 min at 25 °C. During the process, the increase in the absorbance at 420 nm was measured in a UV-2450 spectrophotometer. The molar extinction coefficient of ABTS is 36,000  $\text{dm}^3/\text{mol}$  per cm. One activity unit was defined as the amount of enzyme required to catalyze 1  $\mu\text{mol}$  of substrate per min. Kinetic tests were performed by measuring the initial reaction rates of the immobilized laccase using different concentrations of ABTS as a substrate in 0.1 M tartaric acid buffer (pH 3.0) at 25 °C. The  $K_m$  values were calculated by linear regression according to the Lineweaver-Burk relationship.

### Determination of stabilities

Free and immobilized laccase were incubated at 55 °C for variable periods in the phosphate buffers at pH = 7.0. The samples

were withdrawn every 30 minutes and their residual activity was immediately assayed to determine their thermal stability.

The storage stabilities of the free and immobilized laccase were evaluated by storing them at 4 °C for 1 month and their residual activities were measured every 3 days.

In order to assess the operating stability of immobilized laccase, several consecutive operating cycles using magnetic field were performed by oxidizing ABTS. At the end of each oxidation cycle, the immobilized laccase (15 mg) was washed three times with PBS (pH = 7) and the procedure was repeated with a fresh aliquot of substrate (Davis S et al 1992).

## Results and discussions

### Characterization of the composites

In the FTIR spectra of ZnTAPc- $\text{Fe}_3\text{O}_4$  nanoparticle composite, the peaks at 1610, 1340, 1080  $\text{cm}^{-1}$  corresponded to the stretching vibrations of C-C and C-N of the ZnTAPc plane. The stretch vibrations of C=N and N-H of amino group were found at 1610  $\text{cm}^{-1}$  and 3360  $\text{cm}^{-1}$ , respectively. The characteristic absorption peak of  $\text{Fe}_3\text{O}_4$  also appeared around 580  $\text{cm}^{-1}$ . The rather strong peak at 880  $\text{cm}^{-1}$  indicated the formation of Zn-O bond, showing the more effective complex between ZnTAPc and  $\text{Fe}_3\text{O}_4$  nanoparticles than that between Cu and  $\text{Fe}_3\text{O}_4$  nanoparticles (Jun et al 2006).

Figure 2 shows the XRD (X-ray diffraction) patterns of ZnTAPc and the ZnTAPc- $\text{Fe}_3\text{O}_4$  nanoparticle composite. The main peaks in the XRD of the composite at  $2\theta = 35.5^\circ, 56.9^\circ, 62.3^\circ$  were characteristics of  $\text{Fe}_3\text{O}_4$  and no character of ZnTAPc was observed. However, when 3% (w/v) ZnTAPc was mixed mechanically with  $\text{Fe}_3\text{O}_4$  nanoparticles, both the characters of ZnTAPc and  $\text{Fe}_3\text{O}_4$  could be observed in the XRD of the mixture (the results are not shown). These results indicated that ZnTAPc dispersed randomly on the surface of  $\text{Fe}_3\text{O}_4$  nanoparticles in the composite to form the molecular dispersion layers (Jian et al 2001).

EDS measurements were performed to analyze the elementary composition of the composite surface, as shown in Figure 3 and Table 1. As expected, the EDS spectrum exhibited the peaks of carbon and nitrogen, indicating that the composite contains the organic compound ZnTAPc. From the ratio of peak areas, corrected for their sensitivity, it could be estimated that the content of carbon is 2.17%, which was higher than the calculated value. This result could be regarded as evidence that most of the ZnTAPc were bonded on the surface of the  $\text{Fe}_3\text{O}_4$  nanoparticles.

Figure 4 exhibits the transmission electron microscopy (TEM) micrograph of the ZnTAPc- $\text{Fe}_3\text{O}_4$  nanoparticle com-

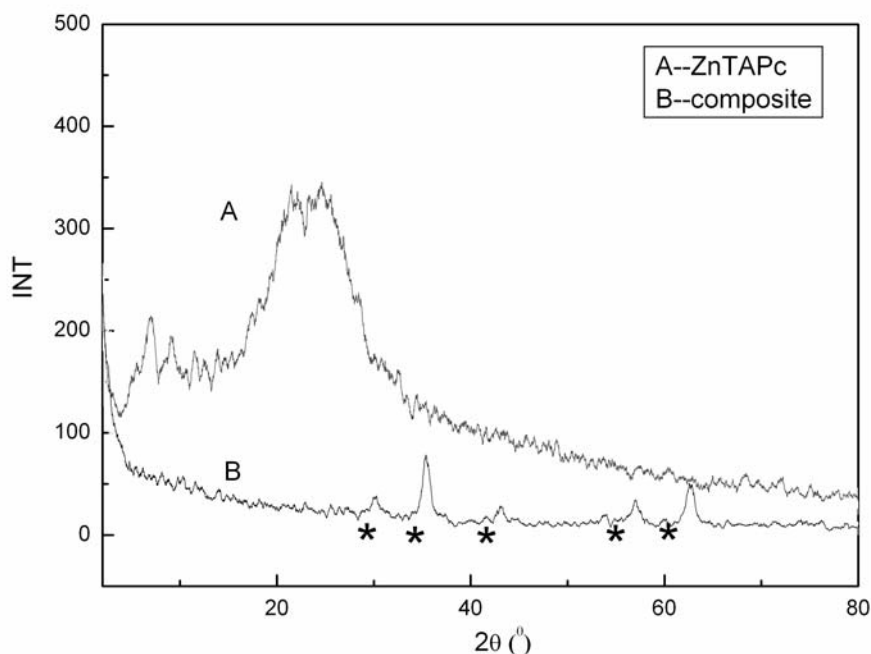


Figure 2 XRD patterns of ZnTAPc and composite.

posite, showing that the particles were roughly spherical. The size analysis demonstrated the average diameter of 15 nm for the composite.

The complex mechanism of the ZnTAPc-Fe<sub>3</sub>O<sub>4</sub> nanoparticle composite was similar to that of the CuPc-Fe<sub>3</sub>O<sub>4</sub> composite (Huang et al 1999). First, the Zn<sup>2+</sup> of ZnTAPc was attached to the O ion of Fe<sub>3</sub>O<sub>4</sub> nanoparticle by chemical bonding action. Then Fe<sub>3</sub>O<sub>4</sub> nanoparticles combined to form large aggregations and ZnTAPc had the function of cohering Fe<sub>3</sub>O<sub>4</sub> nanoparticles. A considerable number of ZnTAPc combined with Fe<sub>3</sub>O<sub>4</sub> nanoparticles on the surface of the

aggregations to form ZnTAPc-Fe<sub>3</sub>O<sub>4</sub> nanoparticle composite. Inside the composite the Fe<sub>3</sub>O<sub>4</sub> nanoparticles accumulated without order, while on the surface of the composite, ZnTAPc formed a molecular dispersion layer.

The surface area was calculated according to Muti-point BET as showed in Figure 5. According to the result, the surface area of the composite was 115.3 m<sup>2</sup>/g, indicating that ZnTAPc-Fe<sub>3</sub>O<sub>4</sub> nanoparticle composite had large surface area for immobilizing enzyme, protein and other biomolecules.

The magnetic characteristic of ZnTAPc-Fe<sub>3</sub>O<sub>4</sub> nanoparticle composite is shown in Figure 6. The composite was almost superparamagnetic and has the Hc of 4.03 Oe. The low coercive force might be caused by the small size of Fe<sub>3</sub>O<sub>4</sub> particles (about 10 nm). As the support of the immobilized

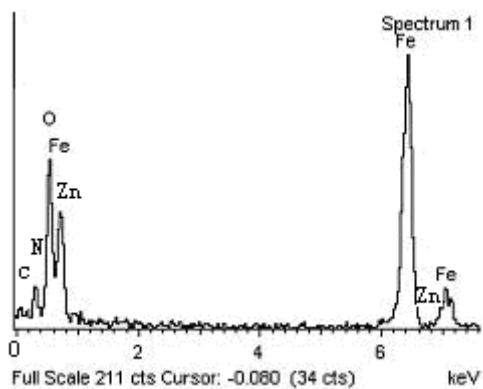
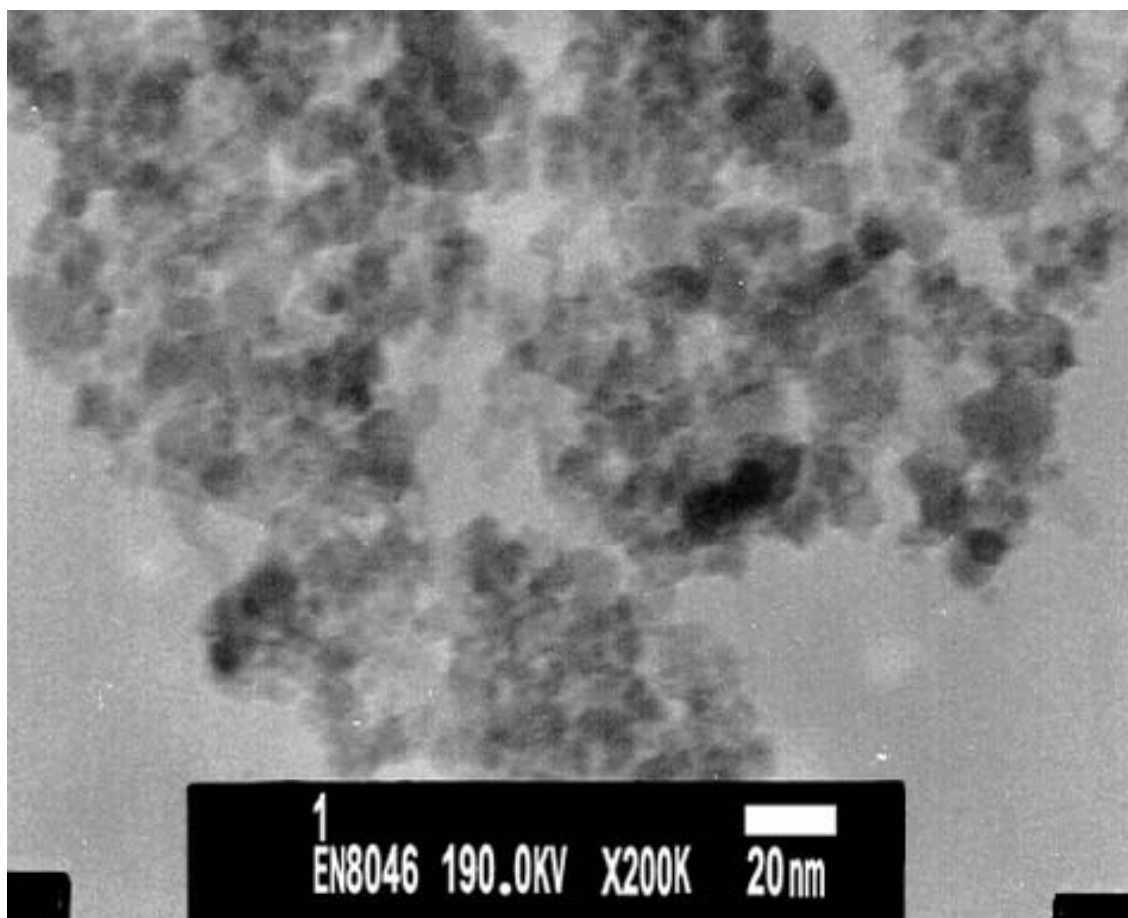


Figure 3 EDS spectrum of the ZnTAPc-Fe<sub>3</sub>O<sub>4</sub> nanoparticle composite.

Table I The result of EDS (the content by weight and atomic percent)

Element	Weight%	Atomic%
O	37.16	63.71
Fe	59.33	29.16
C	2.16	4.93
Zn	0.28	0.11
N	1.07	2.09
Totals	100.00	100.00



**Figure 4** TEM pattern of the ZnTAPc-Fe<sub>3</sub>O<sub>4</sub> composite.

protein, the small Hc was very advantageous to their separation from solution and reuse.

The black Fe<sub>3</sub>O<sub>4</sub> nanoparticles can be oxidized into yellow Fe<sub>2</sub>O<sub>3</sub> when they are exposed to the air directly and their magnetism decreases significantly. However, after six months storage when exposed to air at room temperature, the color and the magnetic properties of the ZnTAPc-Fe<sub>3</sub>O<sub>4</sub> nanoparticle composites remained almost unchanged. As the majority of the ZnTAPc was attached to the surface of the composite, the Fe<sub>3</sub>O<sub>4</sub> nanoparticles were shielded from oxygen and the stability of the Fe<sub>3</sub>O<sub>4</sub> nanoparticles was greatly improved. This kind of composite had very good storage stability.

### Immobilization of laccase

In the composite, the amino groups of the organic compound exposed outside were active groups, which could covalently bond with glutaraldehyde to form Schiff's base, then terminal aldehydic group of glutaraldehyde could covalently bond laccase as showed in Figure 7.

### Properties of immobilized laccase

The effects of pH on the activity of the free and immobilized laccase are shown in Figure 8. The optimal pH for the free and immobilized laccases were the same at pH 3.0. In general, immobilization of enzymes on charged supports often leads to displacements of the pH-activity profile to either alkaline or acidic regions (D'Annibale et al 1999; Leontievsky et al 2001). However, in the present study, the pH-activity profile of immobilized laccase was similar to that of the free counterpart. Therefore, it can be inferred that the immobilization process had little effect on the microenvironment of laccase molecule. This result agreed with those of previous researchers (D'Annibale et al 1999).

The temperature dependence of activity of free and immobilized laccase is shown in Figure 9. The optimal temperature for the laccase immobilized on ZnTAPc-Fe<sub>3</sub>O<sub>4</sub> nanoparticle composite was 45 °C, 10 °C lower than that for the free laccase. For the purpose of calculation, laccase activity observed at optimal temperature was taken as 100%. As the

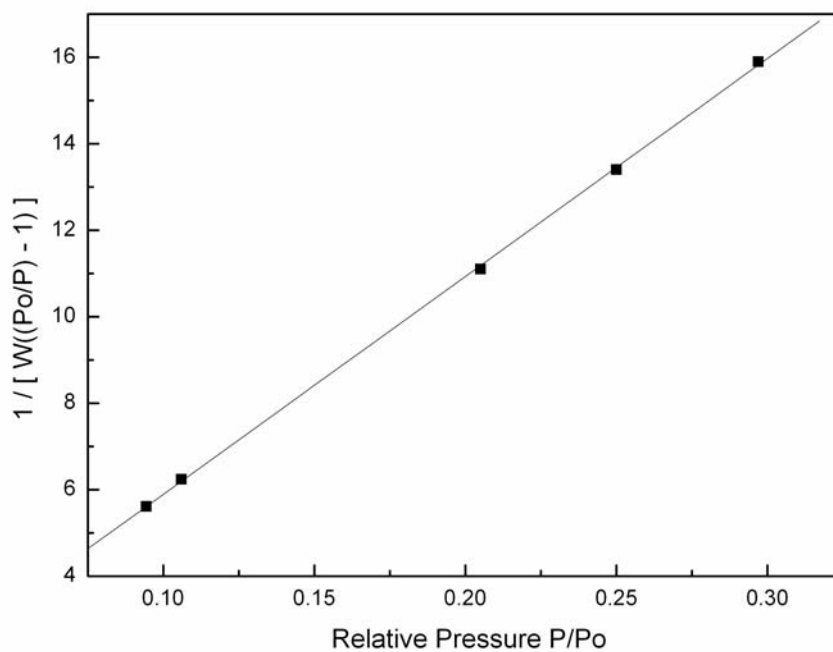


Figure 5 Multi-point BET plot of the ZnTAPc-Fe<sub>3</sub>O<sub>4</sub> nanoparticle composite.

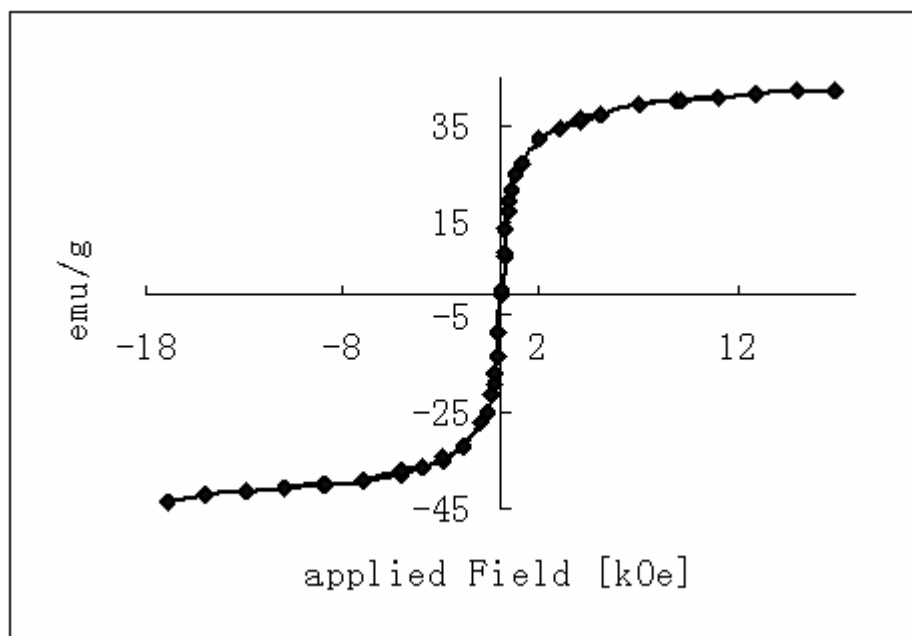


Figure 6 Hysteresis Loop of ZnTAPc-Fe<sub>3</sub>O<sub>4</sub> nanoparticle composite.

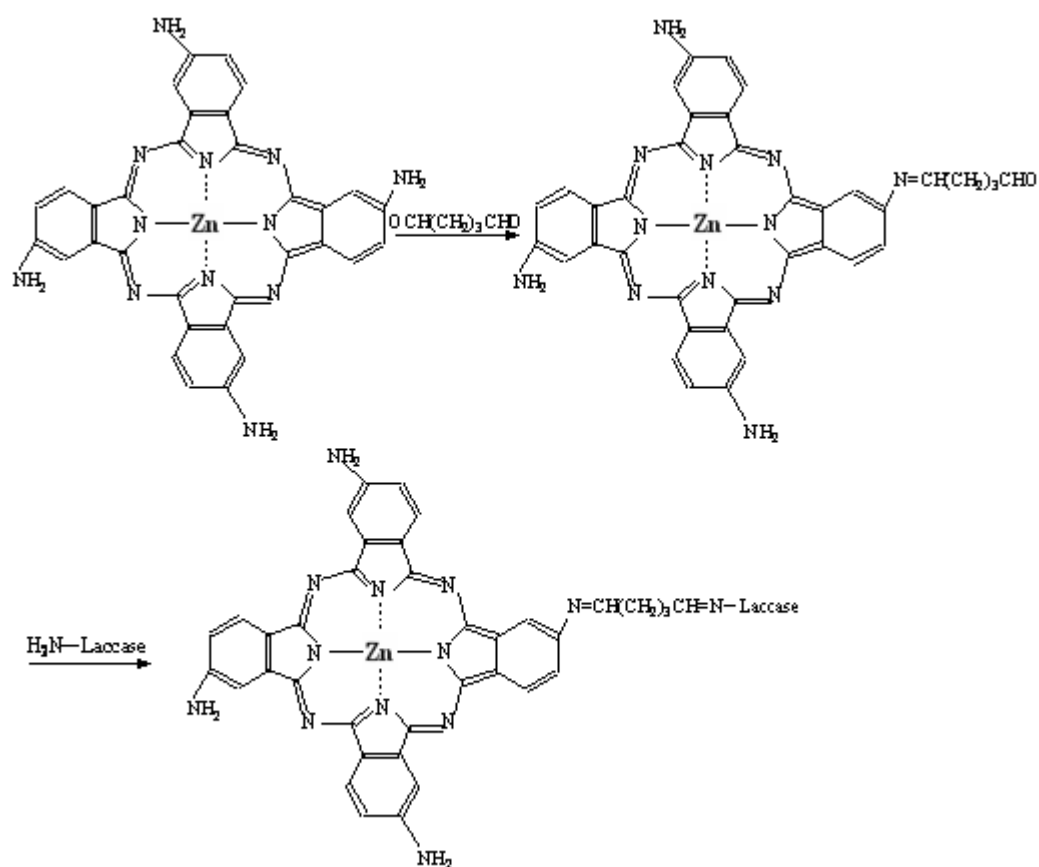


Figure 7 Schematic illustration of laccase immobilized on ZnTAPc- $\text{Fe}_3\text{O}_4$  nanoparticles.

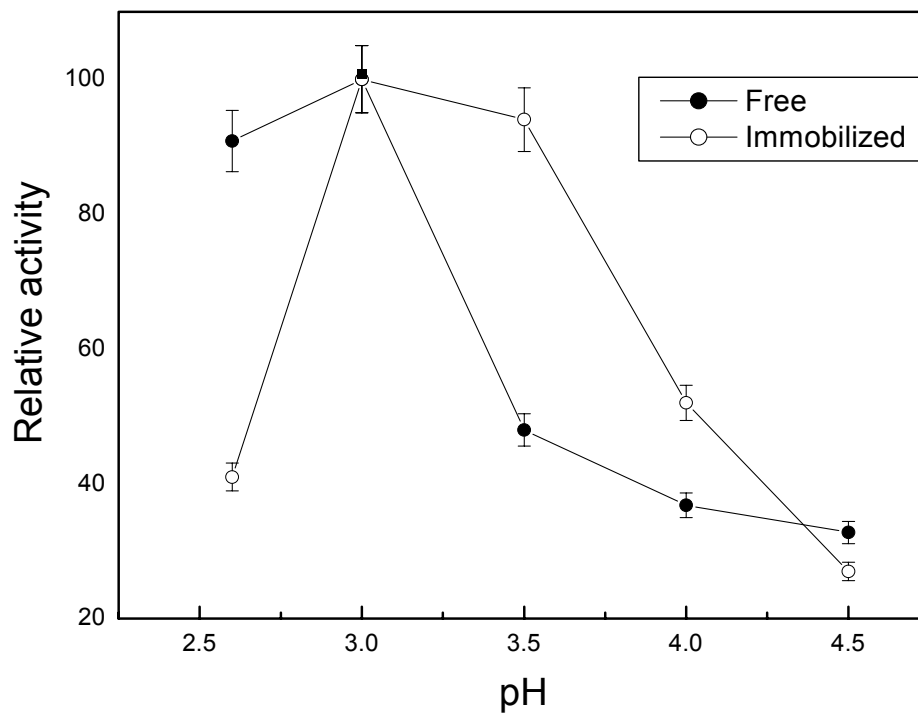


Figure 8 Effect of pH on activities of laccases.

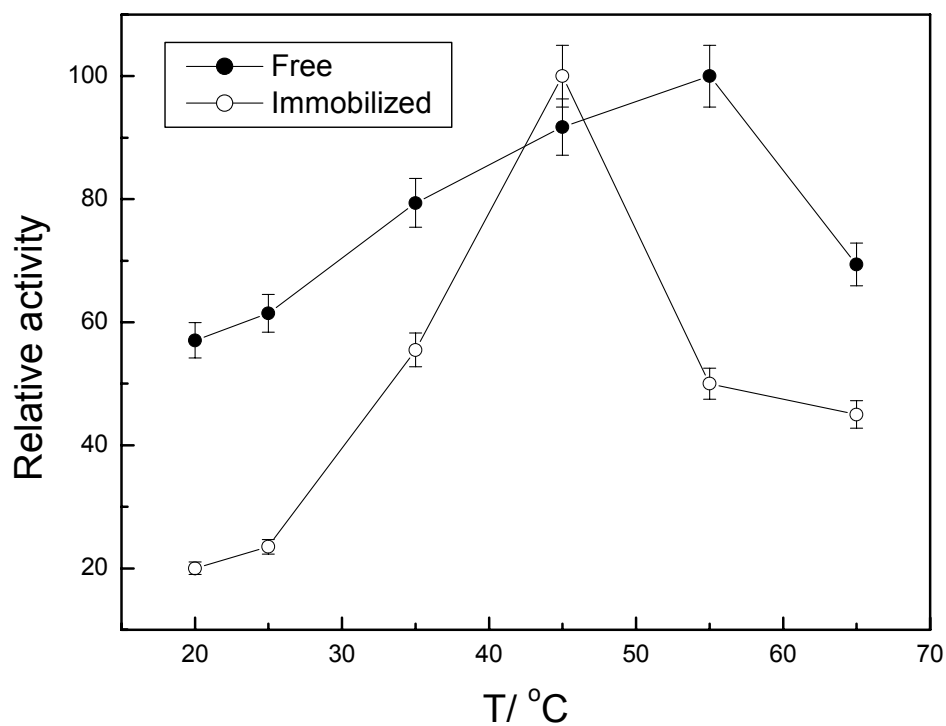


Figure 9 Effect of temperature on activities of laccase.

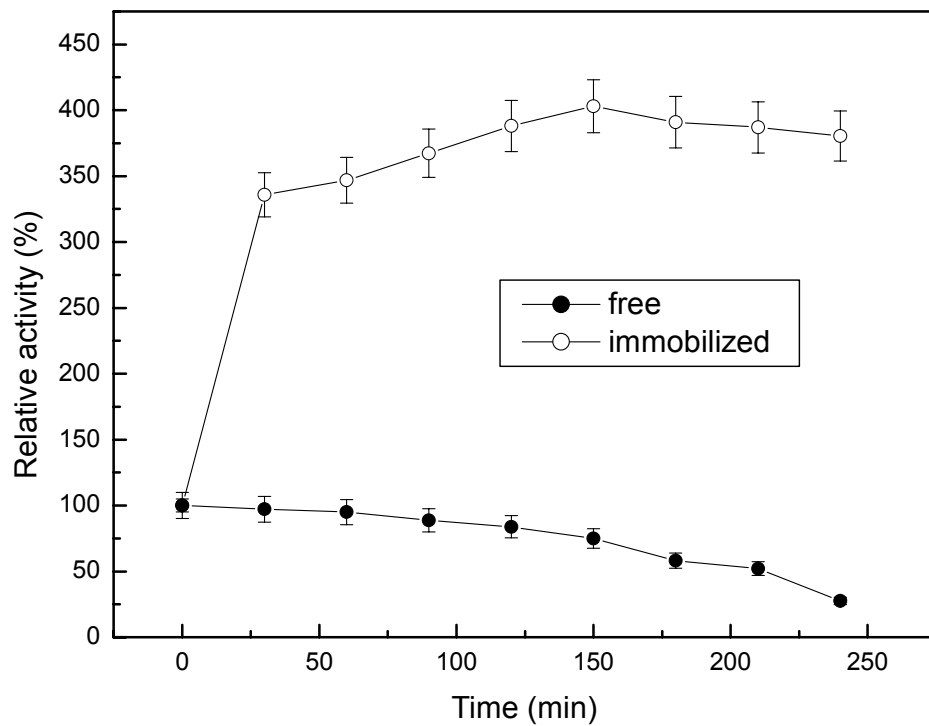


Figure 10 Thermal stabilities of free and immobilized laccase.



temperature decreased to 25 °C, the free laccase displayed a relative activity of 61%, whereas the activity of immobilized laccases dropped significantly to 21%, indicating that the enzyme activity became more dependent on the temperature after immobilization.

## Kinetic properties of the immobilized laccase

$K_m$  values are the most useful parameters in probing the ability of an enzyme to bind its substrate. The Michaelis–Menten constants of free and immobilized enzyme for ABTS were 12.6  $\mu\text{M}$  and 20.1  $\mu\text{M}$ , respectively. The increase of  $K_m$  might be caused by many factors such as steric hindrance of the active site by the support, the loss of enzyme flexibility necessary for substrate binding and the diffusion limitation of substrate (Çetinus et al 2003). However, a decrease in the  $K_m$  value of immobilized laccase was observed compared to the previous  $K_m$  value (23.8  $\mu\text{M}$ ) obtained using CuTAPc as the support (Jun H et al 2006). It can be inferred that the lower diameter of immobilized laccase may lead to a higher affinity towards the substrate, and smaller particle would give less restriction for diffusion.

## Stability of the immobilized laccase

The free and immobilized laccase were both incubated at 55 °C for 240 min in the phosphate buffers at pH = 7.0 to determine the thermal stability (Figure 10). The results showed that the activity of immobilized enzyme increased quickly to 4 times of its initial value at first 150 min and then reached a approximately steady state in the following 90 min, while that of the free laccase decreased significantly to 28% of its initial value after 240 min of incubation. These results agree with those of Abdulkareem et al (2002), who reported on temperature stabilities for laccase immobilized on modified cellulose and acrylic carriers. This could be explained in terms of activation-period inactivation. The immobilization limited enzyme to undergo drastic conformational changes, thus resulting in increased stability towards denaturation (Klibanov 1979; Joon et al 2000; De et al 2004). The outstanding thermal stability of immobilized laccase in this work was the principal advantage over the other immobilized laccase reported before (D'Annibale et al 1999; Abdulkareem et al 2002).

After the immobilized laccase were reserved at 4 °C for 1 month, their activity declined slowly to 85% of initial activity. Under the same storage conditions, activity of free laccase decreased to 30% after 1-month storage. The results show that immobilized laccase has better storage stability than free laccase.

After 5 consecutive operations, the immobilized laccase retained 80% residual activity and displayed good reusability.

## Conclusions

ZnTAPc- $\text{Fe}_3\text{O}_4$  nanoparticle composite with the mean size of 15nm were prepared and characterized. There was an effective complex between ZnTAPc and  $\text{Fe}_3\text{O}_4$  nanoparticles, and the composite was a good carrier for laccase immobilization. The optimal pH for the activity of the immobilized laccases and free laccase were both at pH 3.0 and the optimal temperature for laccase immobilization on ZnTAPc- $\text{Fe}_3\text{O}_4$  nanoparticle composite was 45°. The immobilization yields and  $K_m$  value of the laccase immobilized on ZnTAPc- $\text{Fe}_3\text{O}_4$  nanoparticle composite were 25% and 20.1  $\mu\text{M}$ , respectively. The immobilized laccase had good thermal, storage and operation stability. The results indicated that this kind of immobilized laccase using ZnTAPc- $\text{Fe}_3\text{O}_4$  nanoparticle composite as the carrier might be a good candidate for the sensing biocomponent of fiber optic biosensors.

## Acknowledgments

Funding for this project was provided by the National Natural Science Foundation of China: Project (60377032) and Key Project (60537050).

## References

- Abdulkareem JH, Jolanta B, Beata GM, et al. 2002. Immobilization of wood-rotting fungi laccases on modified cellulose and acrylic carriers. *Process Biochem*, 37:1387–94.
- Arica Y, Yavuz H, Patir D, et al. 2000. Immobilization of glucoamylase onto spacer-arm attached magnetic poly(methylmethacrylate) microspheres: characterization and application to a continuous flow reactor. *Mol Catal B Enzymatic*, 11:127–38.
- Çetinus SA, Öztöp HN. 2003. Immobilization of catalase into chemically crosslinked chitosan beads. *Enzyme and Microbial Technology*, 32:889–94.
- Chen DH, Liao MH. 2002. Preparation and characterization of YADH-bound magnetic nanoparticles. *Mol Catal B Enzymatic*, 16:283–91.
- Cong FD, Du XG, Zhao BZ, et al. 2002. Synthesis and characterization of two positional isomeric tetraamino-phthalocyanines Zinc( $\alpha$ ). *J Chinese Universities*, 23:2221–5.
- Cooper J, Cass A. 2004. *Biosensors*. Oxford :Oxford University Press.
- D'Annibale A, Stazi SR, Vinciguerra V, et al. 1999. Characterization of immobilized laccase from *Lentinula edodes* and its use in olive-mill wastewater treatment. *Process Biochem*. 34:697–706.
- Davis S, Burns G. 1992. Covalent immobilization of laccase on activated carbon for phenolic effluent treatment. *Appl Microbiol Biotechnol*, 37:474–9.
- De Q, Yousung K, Woonsup S. 2004. Characterization of an amperometric laccase electrode covalently immobilized on platinum surface. *J Electroanalytical Chem*, 561:181–9.
- D'souza SF. 2001. Microbial biosensors. *Biosens Bioelectron*, 16:337–53.
- Duran N, Rosa M, D'Annibale A, et al. 2002. Applications of laccases and tyrosinases (phenoloxidases) immobilized on different supports: a review. *Enzyme Microb Technol*, 31:907–31.

- Huang J, Guan J, Yuan R. 1999. Study on  $\text{Fe}_3\text{O}_4$  nanocomplex. *Acta Mater Comp Sinica*, 16:35–9.
- Huang J, Jiang DS, Guan JG, et al. 2001. Complex mechanism of phthalocyanine nickel with  $\text{Fe}_3\text{O}_4$  nano particles and the structure model of the nanoparticles composite. *Acta Mater Comp Sinica*, 18:81–4.
- Jian GG, Jun H, Su LZ, et al. 2001. Characterization and properties of metal phthalocyanine- $\text{Fe}_3\text{O}_4$  nanocomposites for electromagnetorheological fluids. *International Journal of Modern Physics B*, 15:599–609.
- Joon TO, Jung K. 2000. Preparation and properties of immobilized amyloglucosidase on nonporous PS/PNaSS microspheres. *Enzyme Microb Tech*, 27:356–61.
- Jun H, Haiyan X, Bin L, et al. 2006. Immobilization of laccase on copper tetraaminophthalocyanine- $\text{Fe}_3\text{O}_4$  nano composite. *Biotechnol Appl Biochem*, 44:93–100.
- Kishen A, John MS, Lim CS, et al. 2003. A fiber optic biosensor (FOBS) to monitor mutans streptococci in human saliva. *Biosens Bioelectron*, 18:1371.
- Klibanov AM. 1979. Enzyme stabilization by immobilization. *Anal Biochem*, 93:1–25.
- Leontievsky AA, Myasoedova NM, Baskunov BP, et al. 2001. Transformation of 2,4,6-trichlorophenol by free and immobilized fungal laccase. *Appl Microbiol Biotechnol*, 57:85–91.
- Li J, He X, Wu Z, et al. 2003. Piezoelectric immunosensor based on magnetic nanoparticles with simple immobilization procedures. *Anal Chim Acta*, 481:191–8.
- Liu X, Ma Z, Xing J, et al. 2004. Preparation and characterization of amino-silane modified superparamagnetic silica nanospheres. *J Magn Magn Mater*, 270:1–6.
- Zheng G, Shu B, Yan D. 2003. Preparation and characterization of immobilized lipase on magnetic hydrophobic microspheres. *Enzyme Microb Technol*, 32:776–82.